

Simulation of Reverse Swing of the Cricket Ball

D G Pahinkar⁺, J Srinivasan

Department of Mechanical Engineering, Indian Institute of Science, Bangalore-560012, INDIA.

(Received August 21, 2009, accepted October 22, 2009)

Abstract. The simulation of reverse swing in a cricket ball has been undertaken using the Detached Eddy Simulation model. The effect of ball speed and roughness height on the magnitude of reverse swing has been examined. The seam is modeled as a ring with a width of 20 mm and height of 1 mm. The drag and side force have been compared with observations. The numerical simulation of reverse swing provides new insight regarding the factors controlling the reverse swing of the cricket ball.

Keywords: Reverse swing, Detached Eddy Simulation, Turbulent Kinetic Energy.

1. Introduction

The reverse swing of a cricket ball has been considered by many to be a mystery that cannot be explained easily from the known laws of fluid mechanics. The bowlers are unable to achieve the reverse swing consistently in the cricket field. There have been many debates about the mechanisms that lead to reverse swing without a satisfactory resolution. On the other hand, the basic mechanism of normal swing of the cricket ball is well known and understood. With seam inclined to the flow direction, for a smooth cricket ball, the flow on the side where seam faces the flow front becomes turbulent with boundary layer on the opposite side remaining laminar. The magnitude of the normal swing for a smooth cricket ball reduces as the ball speed increases. When the flow on both sides becomes turbulent, there is no normal swing.

There have been several attempts to measure the drag and side force of the cricket ball experimentally. However, difference in experimental observations and actual practice lies in the method used to hold the ball during the measurement. Barton [1] measured side force values for different ball speeds and different conditions like back spin, different seam angles and wobbling. The stability of ball in flight because of back spin, late swing and effect of humidity on swing were also addressed in his thorough experimental investigation. Mehta [2] discussed various fluid dynamics phenomena quantitatively for the flow over cricket ball and also estimated critical speed for transition in this case to be 70 kmph. Bartlett *et al.* [3] studied the biomechanics of fast bowling with different bowling actions and subsequent ball speed for different international and local bowlers. The influence of Fluid Mechanics parameters were also addressed in brief. Binnie [4] studied the effect of humidity on swing. He argued that the increase in magnitude of swing is because of interference of condensation shock with laminar boundary layer at high humidity values. Sayers and Hill [5] measured the drag, lift and side force in a cricket ball at different speeds. Effect of external conditions imposed on the cricket ball in the form of top spin and roughness was documented through variation of the lateral forces. Alam *et al.* [6] studied the drag and lift force variation for different tennis ball speeds with emphasis on lift force variation with different values of rotation per minute. Sayers [7] reproduced the reverse swing of cricket ball through experiments by modeling the cricket ball as sphere with three distinct rings representing the seam. The side force values for different seam angles and different ball speeds were observed. Effect of seam angle on the side force reversal was observed for a particular roughness height. However, we do not have a widely accepted theory to explain the reverse swing of a rough cricket ball.

There has been no study of the reverse swing of a cricket ball swing using the modern tool of computational fluid dynamics. The main focus of this paper is the simulation of the variation of flow around a cricket ball using computational fluid dynamics.

⁺ Corresponding author. Tel.: +91-9960-687-561.
E-mail address: darshan.pahinkar@gmail.com

2. Simulation Methodologies and modeling

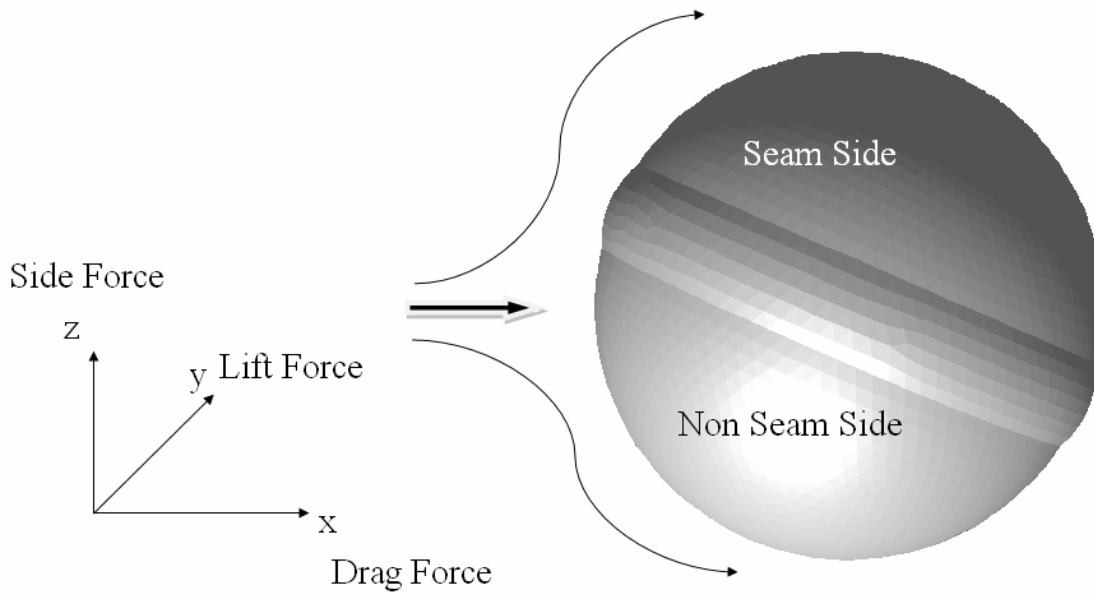


Figure 1: Geometry of the Cricket ball used for simulations and direction of forces

With advent of super-computers it is now possible to study three dimensional problems like the flow over cricket ball with more accuracy. The code used to discretize momentum equations and solve numerically was FLUENT, including GAMBIT. This code was preferred over open FORTRAN codes because of its ability to handle complex geometries. It was earlier found out that the same code was sensitive to change of geometry from smooth sphere to that of cricket ball.

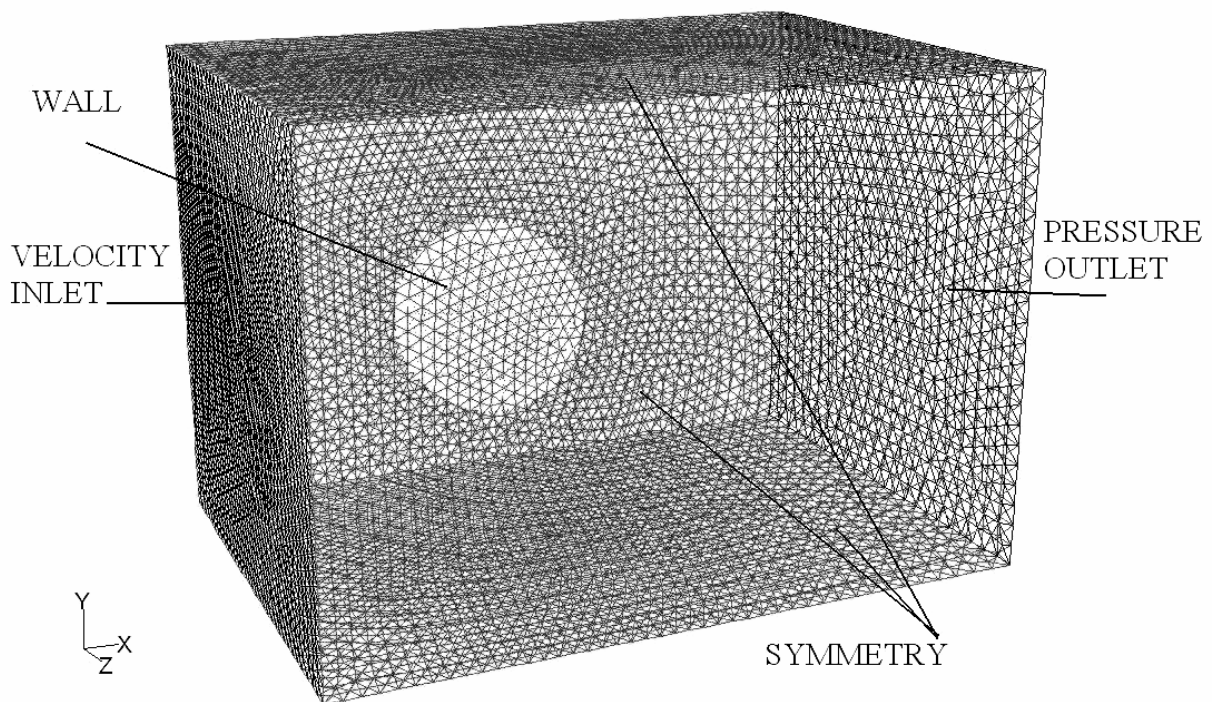


Figure 2: Grid used for simulations and boundary conditions applied.

The Cricket ball was modeled as a sphere of diameter 74 mm with seam 20 mm wide and 1 mm high concentric rim representing seam using GAMBIT 2.2.30. Figure 1 shows the model of the Cricket ball used for simulations which is kept at 30° with respect to air flow direction. Various terms used and direction of

forces are also shown. The domain chosen for simulations was a rectangular parallelepiped $7*D$ long and $5*D$ wide and deep where D is the diameter of the ball. The ball was kept at $2*D$ from the inlet to capture the downstream effects clearly. The grid generated had 14000 points on the surface of ball and 1.4 million control volumes. The ball surface was split into different faces to impart different surface roughness heights.

The Navier-Stokes equations were solved by using Detached Eddy simulation approach available with FLUENT 6.3 which is amalgamation of Spalart-Allmaras model near the wall surface with Large Eddy Simulation (LES) in the far region. Spalart-Allmaras model is a turbulence model which involves solution of Reynolds Averaged Navier-Stokes (RANS) Equations with closure obtained by eddy viscosity transport equation. LES involves spatial averaging of Navier-Stokes Equations. This attribute helps to allow coarser grid to save computational time and cost. Different boundary conditions as shown in figure 2 were imparted on corresponding surfaces and simulations were carried out on 'IBM Regatta' at the Supercomputer Education and Research Centre in Indian Institute of Science.

The model used very near to wall was law of wall or log law. The roughness was modeled by modifying slope of law of wall in such a way that the resultant shear stress is approximately equal to that predicted by Nikrudise's chart [8]. The ultimate effect of this change in velocity profile is reflected in the flow structure around the Cricket ball and separation points.

The value of roughness for an actual rough cricket ball was measured experimentally with a 3-D LASER scanner. The actual cricket ball does not necessarily have same roughness height all over the surface. The roughness height in different patches of the cricket ball varied from 0.15 mm to 1 mm. The value chosen by Sayers [7] in his experiments was 0.3 mm, which was chosen for present cases, so that the ratio of roughness to diameter is 0.004.

3. Results and Discussion

3.1. Flow patterns and angular variation of wall parameters for Ball speed 120 kmph

Figure 3 shows the schematic of the flow pattern during reverse swing based on experiments by Sayers [7]. It was observed in experiments that reverse swing occurs when the velocity of the ball is more than a certain threshold velocity for a particular Seam angle. Value of this threshold velocity is different for different seam angles. We chose one value of seam angle i.e. 30° and carried out simulations for different values of ball speeds and different initial conditions like changing roughness height and adding top spin. Experiments confirm that reverse swing occurs only when smooth side undergoes turbulent separation while the rough side with the seam does not.

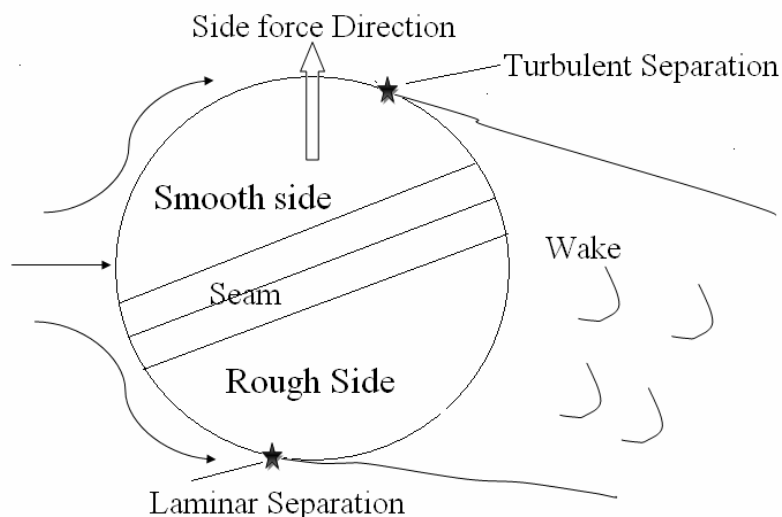


Figure 3: Circumstances required for inception of reverse swing of Cricket ball.

It clear that reverse swing occurs when side force acts in a direction that is opposite to the direction in which the seam points. Figure 4 shows the iso-vorticity contours for flow over a cricket ball at a speed of 33 m/s or 120 kmph with the side behind seam kept rough with the specified value 0.3 mm sand grain type

roughness. As the flow on the smooth side undergoes turbulent separation it disturbs the vortex tube downstream curling the tube into two separate tubes as shown in figure 4. Figures 5 and 6 show the typical vorticity contours in two azimuthal planes which are perpendicular to each other. Figure 6 clearly shows the different types of separation on the seam side and non-seam side in x-z plane. The seam is shown with solid lines in the figure. The vorticity contours show that flow on the seam side has separated earlier than the flow on the non-seam side. This asymmetry caused the flow to be asymmetric downstream causing net side force in the direction opposite to that if the ball had been smooth. Figure 6 shows the vorticity contours in x-y plane. The x-z plane shows asymmetry while the x-y plane shows symmetry about the stream wise direction indicating the lift force is quite small as compared to the side force for the reverse swing.

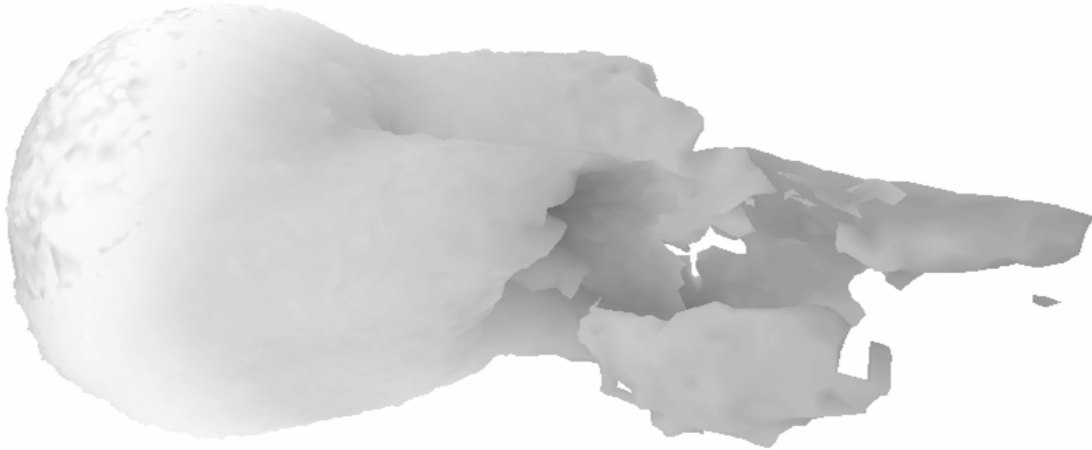


Figure 4: Iso-Vorticity Contours showing vortical structure behind Cricket ball experiencing reverse swing. Upper half is smooth (non seam side) undergoing turbulent separation and flow in lower half (rough) separates early. Curling up of vortices is observed in the upper half.

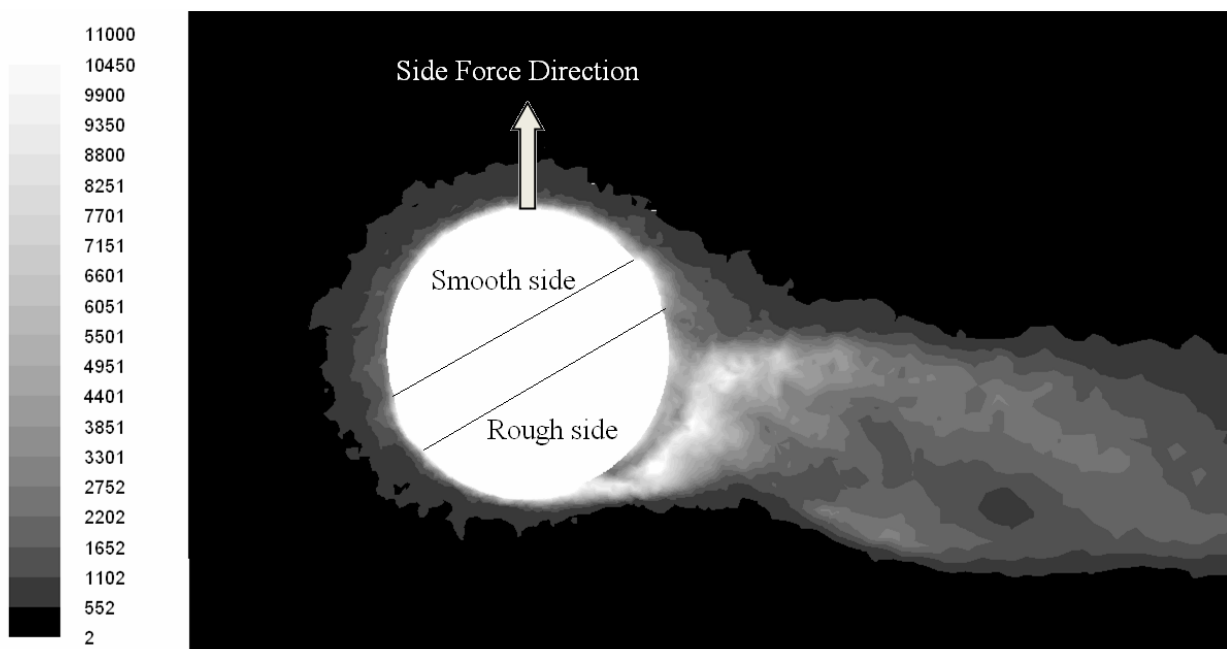


Figure 5: Vorticity Contours for x-z plane showing asymmetric wake region because of earlier separation on rough side and delayed separation on smooth side

The two contour plots can be compared with each other to deduce the effect of roughness on the fluid

dynamics of the cricket ball. Figure 7 shows a detailed view of the flow around Cricket ball on the downstream side. The figure shows velocity vectors that indicate separation on both sides. The flow in lower half of Cricket ball separates early and aids the curling up of vortices generated due to delayed separation in the upper half of the flow. The small vortex in the lower half can be seen, which has its mirror image on the other side of the ball. All this complicated flow structure ultimately deflects the wake region downwards and hence generates the side force in upward direction.

The angular variation of pressure coefficient averaged over time but not averaged over span, plotted in figure 8 supports the vorticity contours in figures 5 and 6. From figure 8 the separation points can be easily noted to be approximately between 100° and 135° . The cluster of points is shown to highlight the fact that not all points in the azimuthal direction undergo separation at the same location. The disturbances in surface pressure can be seen near the location of seam. The earlier separation on seam side and delayed separation on the non-seam side can be seen in figure 8.

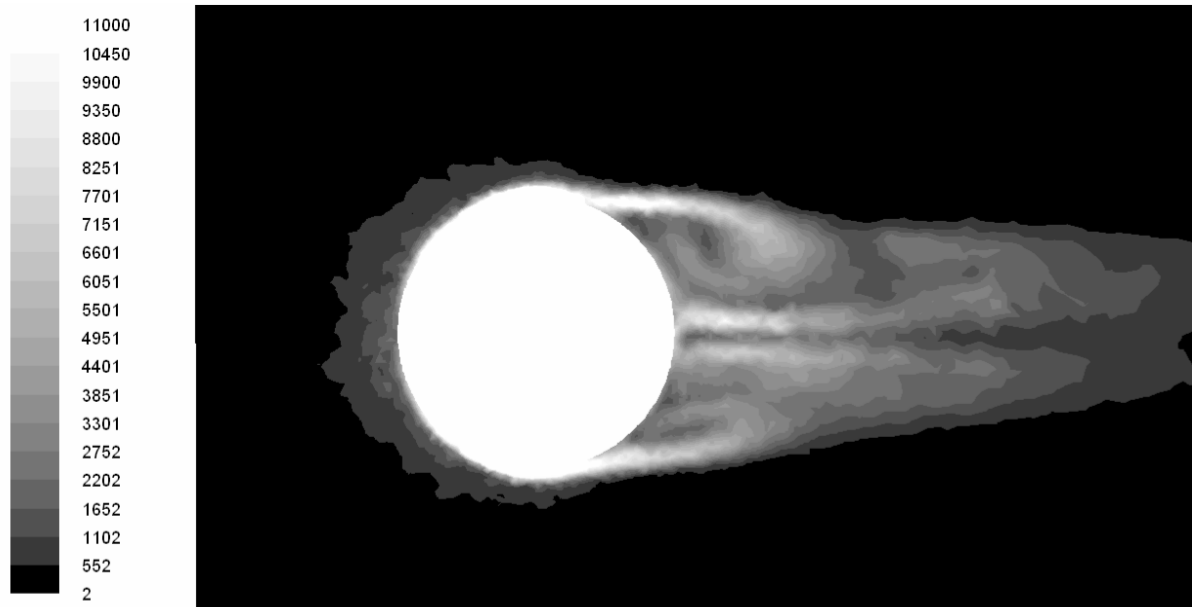


Figure 6: Vorticity Contours for x-y plane showing symmetric wake region as no disparity in geometry is present in this plane

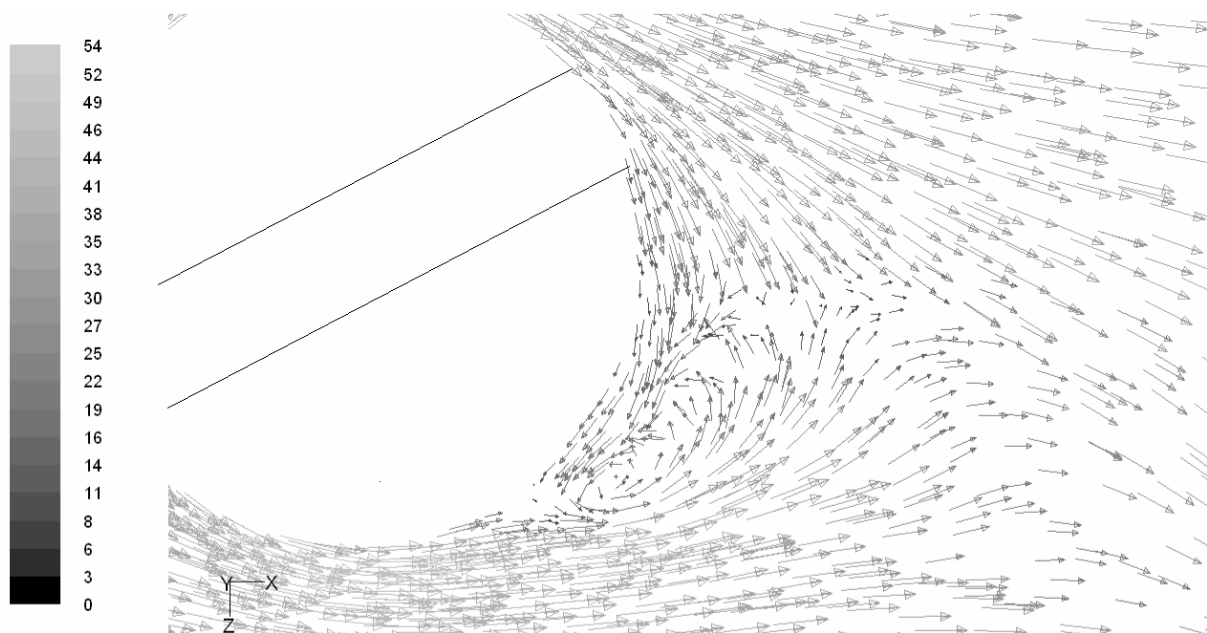


Figure 7: Velocity vectors in x-z plane showing small vortex attached to bottom side of the Cricket ball. Different separations on upper and lower side are also seen.

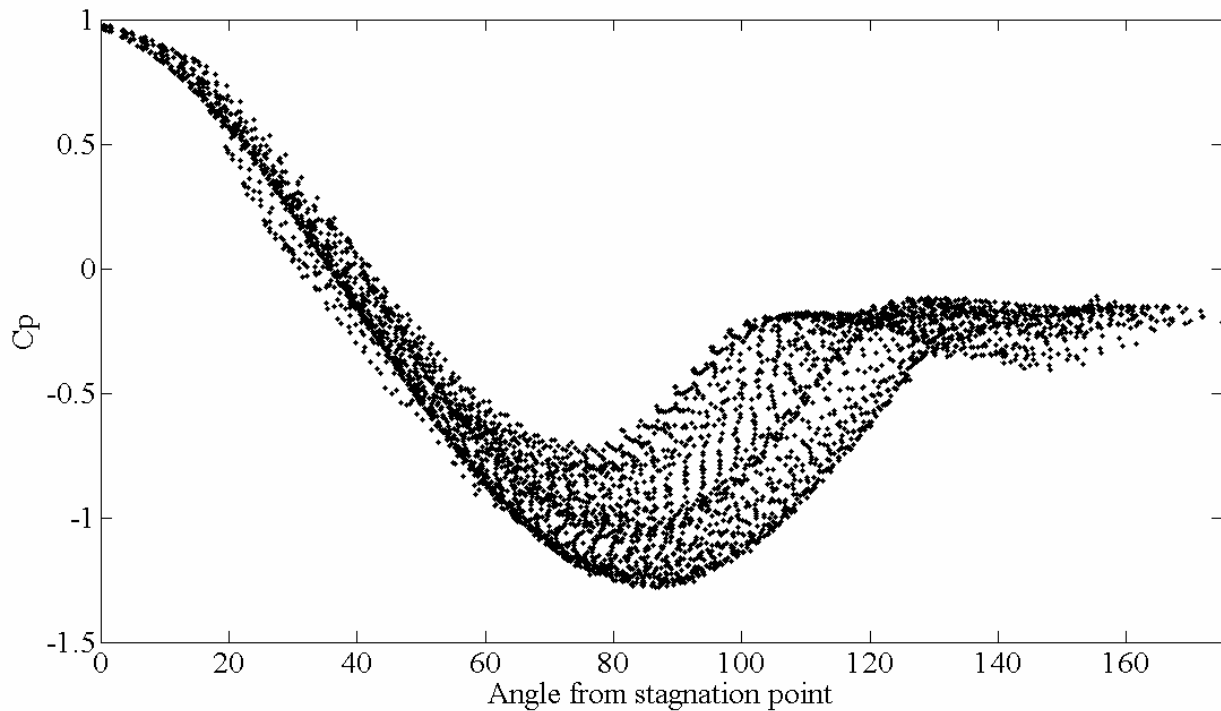


Figure 8: Angular Variation of pressure coefficient for Cricket ball surface showing gradual change of separation points

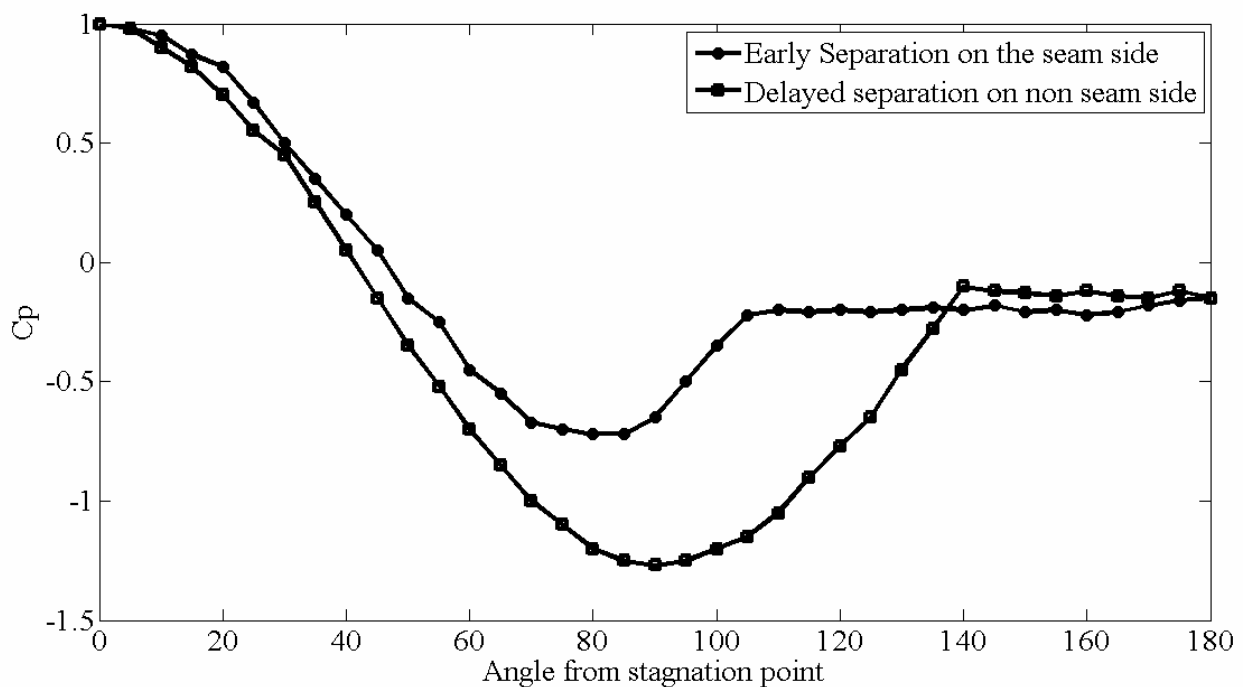


Figure 9: Angular Variation of pressure coefficient for two extreme sides of cricket ball showing earlier and delayed separation on respective sides

To be more precise the pressure coefficient values on the respective extremities can be seen in figure 9, where the C_p values are plotted at every 5° . The angles of separation on two extreme sides are clearly seen in figure 9. Also the base suction coefficients on both sides can be noted as 1.25 and 0.72 on non seam and seam side respectively.

Angular variation of Turbulent Kinetic Energy (TKE) based on RMS value of fluctuating velocity on both the sides is shown in figure 10. This variation corroborates the vorticity contours in figures 5 and 6 and pressure variation in figure 9. TKE on the seam side or rough side shoots up at an angle between 80° and

100° and TKE on the smooth side which undergoes turbulent separation goes up quite late (at around 135°). These results are in agreement with the flow visualizations with woolen tufts by Sayers [7].

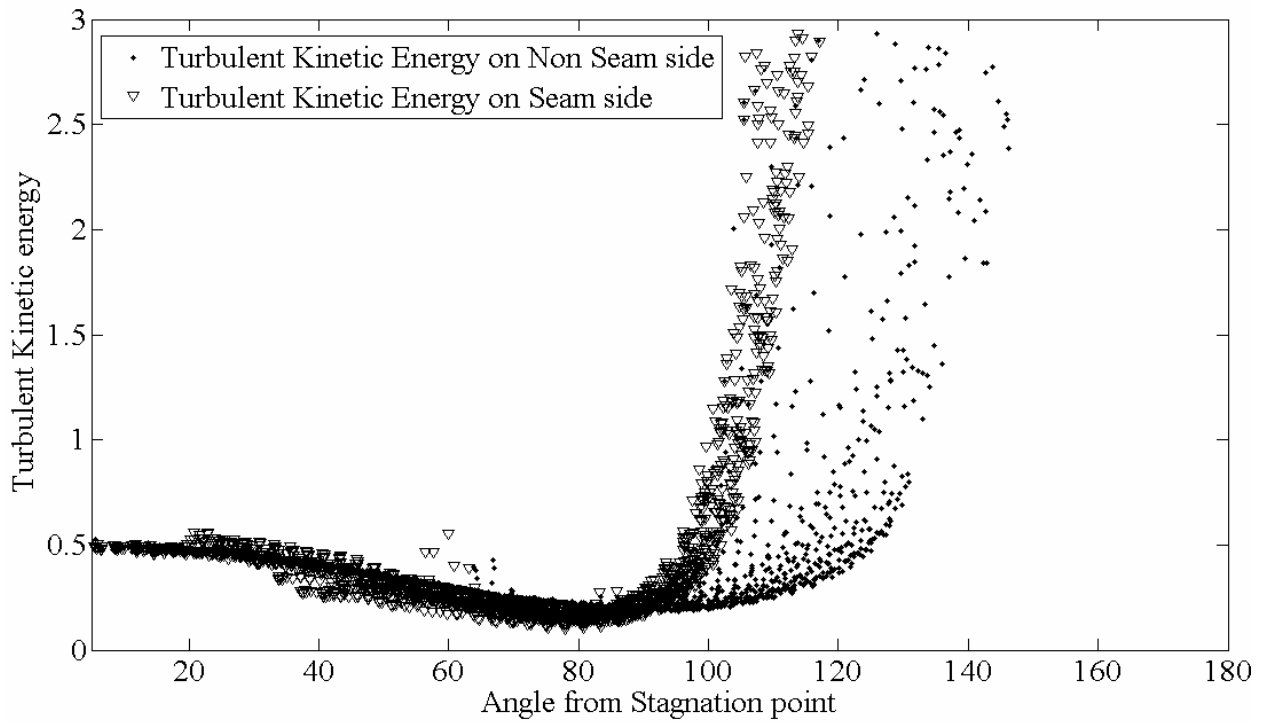


Figure 10: Angular Variation of Turbulent Kinetic Energy for Cricket ball surface with increase in its values at different angular locations on opposite sides.

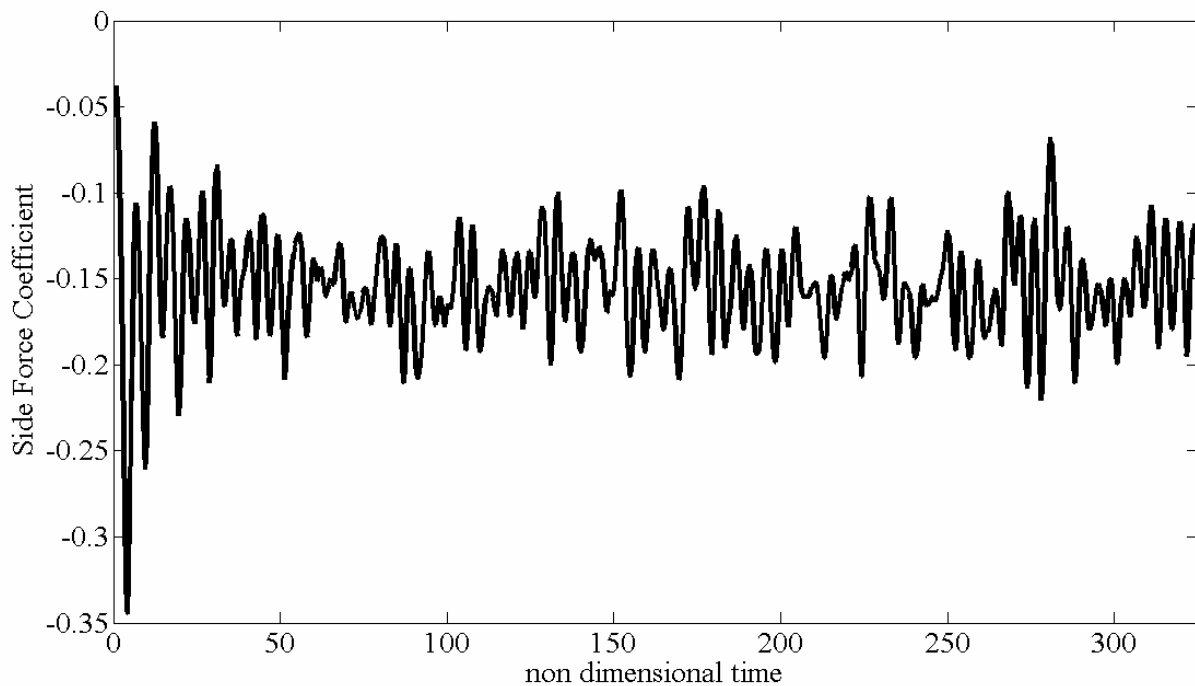


Figure 11: Transient Variation of side force coefficient at cricket ball velocity 33 m/s in case of reverse swing. Amplitude keeps shifting but shedding is orderly.

The transient variation of side force in case of reverse swing was also noted and shedding frequencies were observed from power spectra of the same. The variation of side force for the case of reverse swing at ball velocity 33 m/s or 120 kmph is plotted in figure 11. It is observed that the vortex shedding, though

asymmetric, is orderly. The magnitude of mean side force is negative showing the side force is in direction opposite to that in which seam points. The power spectrum of the side force coefficient variation in figure 11 is plotted in figure 12, which shows the peaks in the range of Strouhal numbers ranging from 0.02 to 0.4 indicating shedding frequencies of the concerned magnitude.

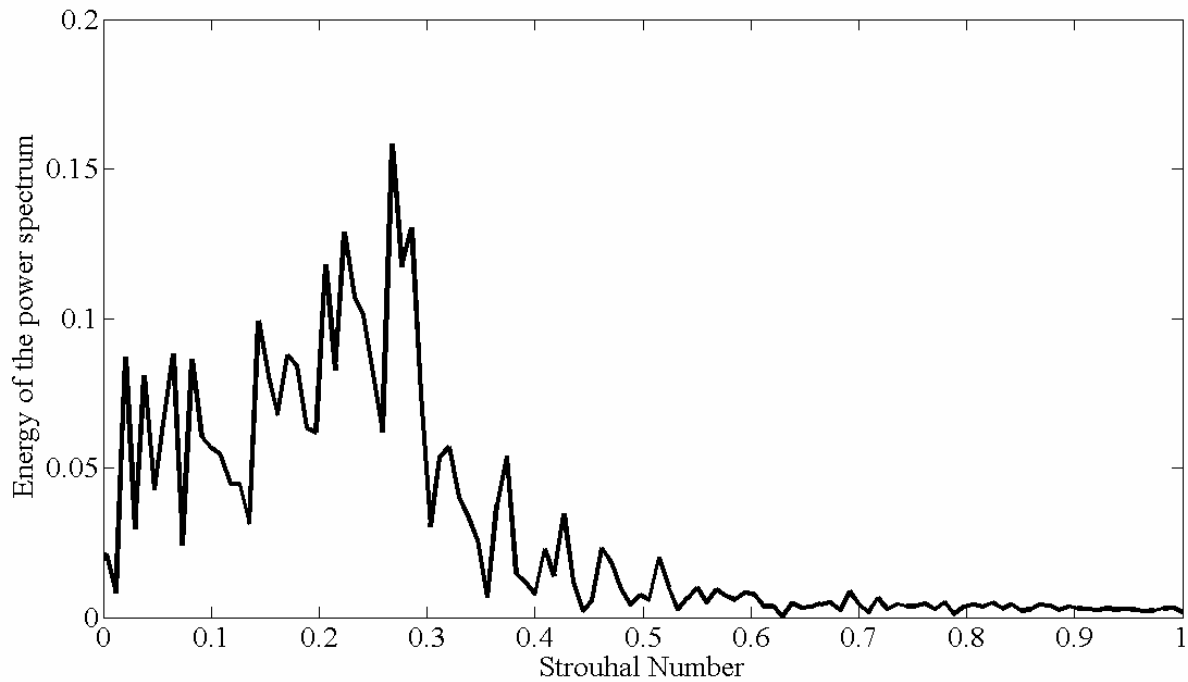


Figure 12: Power Spectrum of side force coefficient at cricket ball velocity 33 m/s in case of reverse swing. Peaks in this graph show shedding frequencies.

3.2. Effect of Cricket ball velocities on magnitude of drag and side forces

The simulations were carried out for different velocities of the cricket ball to study the effect of velocity on magnitude of drag and side force values. The values of drag forces in N were plotted against available data from experiments by Sayers and Hill [7]. Figure 13 shows drag force value for different ball speeds.

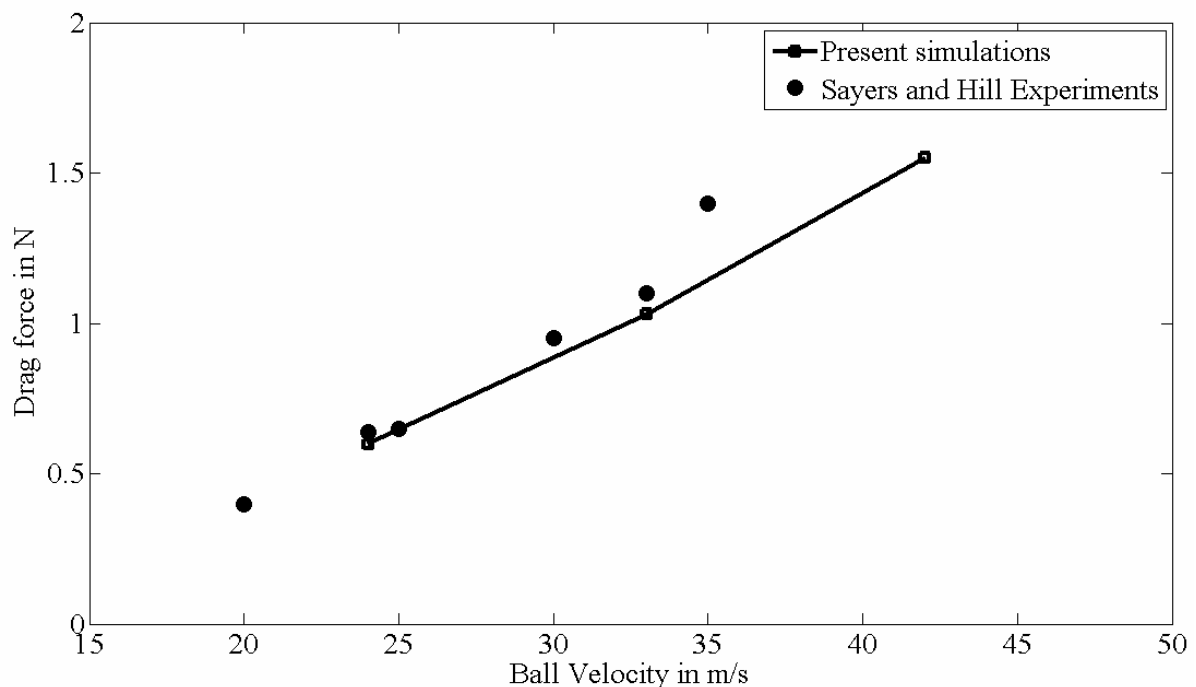


Figure 13: Variation of drag force for Cricket ball undergoing reverse swing for different velocities.

The side force values which are normalized with the standard weight of the Cricket ball i.e. 1.52 N, were simulated for different values of velocities of the cricket ball (rough on one side as shown in figure 3). The impact of back spin was also examined. It is interesting to note that the trend predicted by simulations is in agreement with the experimental values at seam angle 15°. The reason can be speculated to be insensitivity of simulation towards small change in seam angles. The ratio of side force and weight of the cricket ball was termed as swing force ratio by Sayers.

$$\text{Swing Force Ratio} = \frac{\text{Side force in N}}{\text{Weight of ball in N}}$$

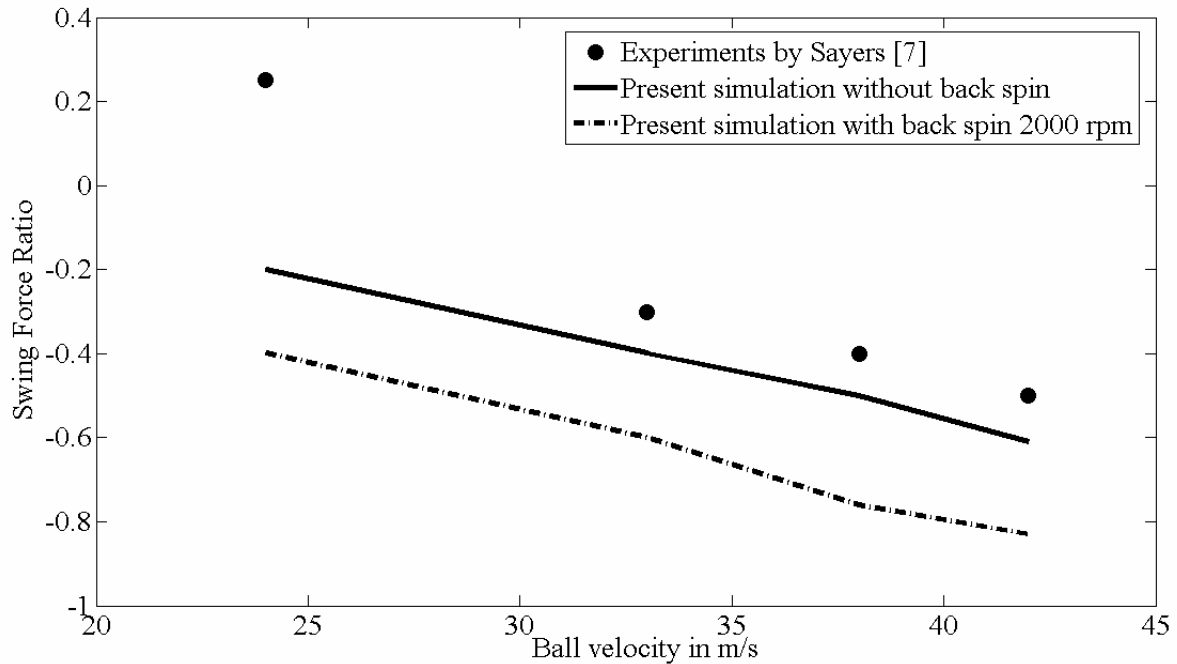


Figure 14: Side force variation for ball with and without back spin for different speeds. The side force reversal observed in experiments was not observed in case of simulations.

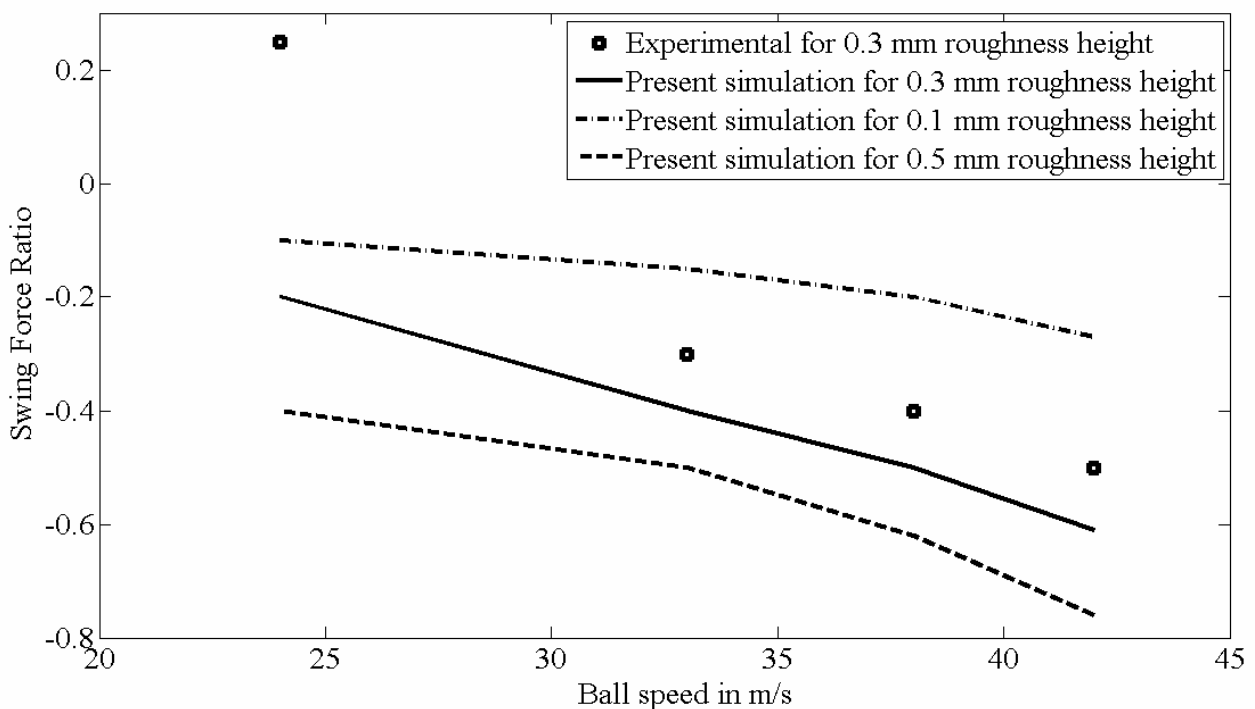


Figure 15: Side force variation for ball with different roughness height for different speeds.

Figure 14 shows the side force variation in terms of swing force ratio with speed for roughness height 0.3 mm, with and without back spin. It was observed that the value of side force increases for corresponding ball velocity if the back spin is imposed on it. It can be inferred from these simulations that back spin helps in getting more side force along with stabilizing the ball trajectory. The reason behind this might lie in skewed axis of rotation with respect to the direction of flow. Also, side force value increases as ball speed increases, supporting the existence of reverse swing at higher speeds with more impact. This trend too was observed in experiments.

One of the limitations of simulation is inability to predict the side force reversal. In reality, reverse swing occurs because of tripped flow on smooth side after a particular threshold velocity. In other words roughness has to overpower the seam to produce the side force in opposite direction to that seam would produce. This phenomenon is dependent on the seam angle, velocity of ball and roughness height. Experimentally it was observed that the side force reversal is advanced with roughness incorporated. The main reason behind absence of the same in present simulation was weaker representation of seam. The seam in experiments by Sayers [7] was modeled by three distinct rings, which was sufficient enough to produce normal swing for pre-critical Reynolds numbers and reverse swing for post critical Reynolds numbers. In the present simulations, due to computational power constraints, seam had to be modeled like a flat rim of standard dimensions. Due to weaker model of seam, roughness height of 0.3 mm, the value used in experiments by Sayers would obviously generate reverse swing.

Even though side force reversal was not able to be captured, effect of change in roughness height was studied. Figure 15 shows swing force ratio for different roughness heights at different ball velocities. It can be seen that for a particular ball speed, roughness increases the side force value in the direction of opposite to that in which seam points. Also side force in each case of roughness heights, side force value increases with ball speed. This trend was similar to that obtained with 0.3 mm roughness height.

The expected flight of the Cricket ball as seen from the top was approximately plotted by using Newton's second law. The ball was assumed to travel a full pitch distance 18 m. The paths calculated for Cricket ball suffering reverse swing for two sample roughness heights are shown in figure 16.

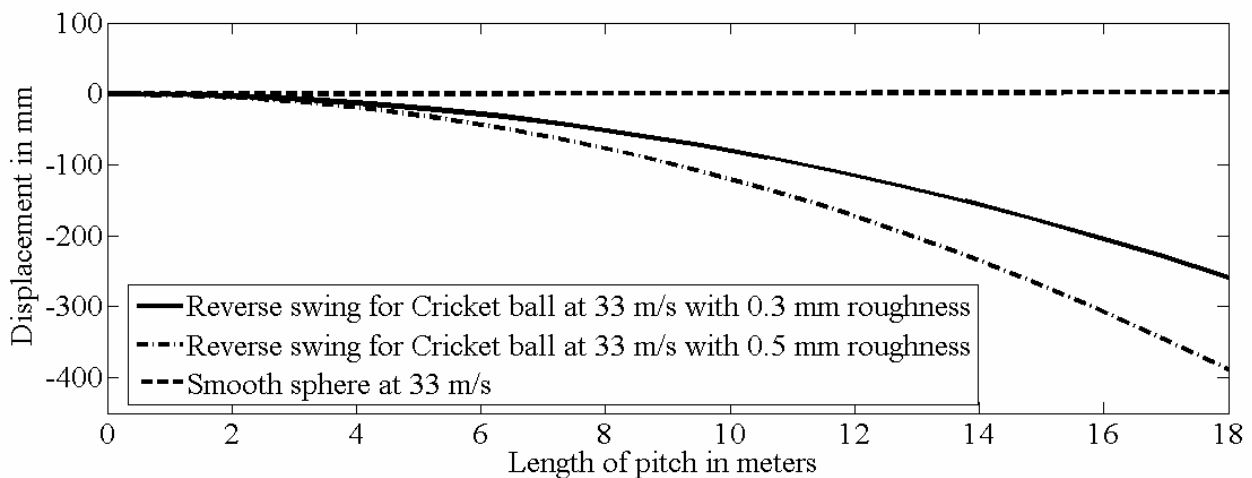


Figure 16: Predicted paths of Cricket ball showing reverse swing at different values of surface roughness.

4. Conclusions

Reverse swing of the Cricket ball was satisfactorily simulated by using DES for different values of ball speeds and roughness height. Reverse swing was found to occur when seam side of the ball underwent laminar separation and likewise, with base suction coefficient 0.72 and 1.25 respectively on either sides. The separation points lie in the range of $80-100^\circ$ for seam side and $120-140^\circ$ for non seam or smooth side. Also transient nature of side force was periodic if not asymmetric for the case of reverse swing, which can be concurrent with the idea that widened wake region, is inefficient to damp the fluctuations in it. In addition to this, it is well known that narrow wake region corresponding to turbulent separation entails no vortex shedding. Side force values for the case of reverse swing increased with ball speed and roughness height. In addition back spin imposed on the rough ball was found to increase the side force. Paths of the rough cricket ball predicted the magnitude of swing for different roughness height to be 26 cm and 39 cm. These values are in reasonable agreement with observations. The present simulations can have a limitation as far as

modeling of seam is concerned. The manufacturing variability in shape of the ball was neglected.

5. Acknowledgements

Authors would like to thank Super computer Education and Research Centre (SERC) of Indian Institute of Science for providing high performance computing resources.

6. References

- [1] N.G. Barton. On the Swing of a cricket ball in flight. *Proceedings of Royal Society London*. 1982, **379**: 109-131.
- [2] R.D. Mehta. Aerodynamics of sports balls. *Annual Rev. Fluid Mechanics*. 1985, **17**: 151-189.
- [3] R.M. Bartlett, N.P. Stockill, B.C. Elliot, A.F. Burnett. The biomechanics of fast bowling in Men's cricket: a Review. *Journal of Sports Science*, 1996, **14**: 403-424.
- [4] A.M. Binnie. Effect of humidity on swing of Cricket balls. *International Journal of Mechanical Sciences*. 1976, **18**: 497-499.
- [5] A.T. Sayers, A. Hill. Aerodynamics of a Cricket ball. *Journal of Wind Engineering and Industrial Aerodynamics*. 1999, **79**: 169-182.
- [6] F.Alam, W.Tio, S.Watkins, A.Subic and J. Naser. Effect of spin on tennis ball aerodynamics: an experimental and computational study. *16th Australasian Fluid Mechanics Conference*. 2007, pp. 324-327.
- [7] A.T. Sayers. On the reverse swing of a cricket ball-modeling and measurements. *Proc. Instn. Mech. Engrs*. 2001, **215**: 45-55.
- [8] FLUENT 6.2 Documentation. User Guide.
- [9] P. Kundu and E. Cohen. *Fluid Mechanics*(Third edition). Academic press.

